

Perforin and Gamma Interferon-Mediated Control of Coronavirus Central Nervous System Infection by CD8 T Cells in the Absence of CD4 T Cells

Cornelia C. Bergmann,^{1,2} Beatriz Parra,^{3†} David R. Hinton,² Chandran Ramakrishna,¹
Konechi C. Dowdell,^{1‡} and Stephen A. Stohlman^{1,2,3*}

Departments of Neurology,¹ Pathology,² and Molecular Microbiology and Immunology,³ Keck School of Medicine, University of Southern California, Los Angeles, California 90033

Received 17 August 2003/Accepted 3 November 2003

Infection of the central nervous system (CNS) with the neurotropic JHM strain of mouse hepatitis virus produces acute and chronic demyelination. The contributions of perforin-mediated cytotoxicity and gamma interferon (IFN- γ) secretion by CD8⁺ T cells to the control of infection and the induction of demyelination were examined by adoptive transfer into infected SCID recipients. Untreated SCID mice exhibited uncontrolled virus replication in all CNS cell types but had little or no demyelination. Memory CD8⁺ T cells from syngeneic wild-type (wt), perforin-deficient, or IFN- γ -deficient (GKO) donors all trafficked into the infected CNS in the absence of CD4⁺ T cells and localized to similar areas. Although CD8⁺ T cells from all three donors suppressed virus replication in the CNS, GKO CD8⁺ T cells expressed the least antiviral activity. A distinct viral antigen distribution in specific CNS cell types revealed different mechanisms of viral control. While wt CD8⁺ T cells inhibited virus replication in all CNS cell types, cytotoxic activity in the absence of IFN- γ suppressed the infection of astrocytes, but not oligodendroglia. In contrast, cells that secreted IFN- γ but lacked cytotoxic activity inhibited replication in oligodendroglia, but not astrocytes. Demyelination was most severe following viral control by wt CD8⁺ T cells but was independent of macrophage infiltration. These data demonstrate the effective control of virus replication by CD8⁺ T cells in the absence of CD4⁺ T cells and support the necessity for the expression of distinct effector mechanisms in the control of viral replication in distinct CNS glial cell types.

Central nervous system (CNS) infections with the neurotropic JHM strain of mouse hepatitis virus (JHMV) induce acute encephalomyelitis in adult mice (10, 13–17, 33). Acute JHMV replication is predominantly controlled by virus-specific CD8⁺ T cells which peak within the CNS concomitant with viral clearance (3, 4, 19). CD8⁺ T cells exert various antiviral functions, including perforin-, tumor necrosis factor alpha-, and Fas/FasL-mediated cytotoxicity (11, 41). CD8⁺ T cells are also a major source of gamma interferon (IFN- γ) (9, 11, 27, 41), which contributes to the resolution of acute viral infections as well as to protection during viral persistence (7, 14, 37). IFN- γ has a direct antiviral action and influences the immune response in multiple ways, including upregulation of major histocompatibility complex (MHC) molecule expression (9, 21, 27, 30, 39). JHMV-specific CD8⁺ T cells within the CNS exhibit perforin-dependent *ex vivo* cytotoxic activity only during acute infections (3, 4, 25); however, they persist and continue to secrete IFN- γ during chronic infections (3, 17–20). This regulation of effector functions may reflect the host's attempt to control acute viral infections while reducing CNS immunopathology. Despite the clearance of infectious virus within 2

weeks, the net outcome is an inability to provide sterile immunity within the CNS, resulting in the persistence of viral antigens and RNA, accompanied by continued myelin loss (10, 15, 19, 35).

During acute encephalomyelitis, JHMV replicates in astrocytes, oligodendroglia, microglia, the resident CNS macrophage population, and CNS-infiltrating macrophages (38). Although a number of JHMV strains also infect neurons, neuronal infections are associated with lethality (10, 15). JHMV isolates with minimal neuronal tropism are thus chosen to study the immune responses controlling acute and subsequent persistent infections associated with chronic demyelination (10, 15, 18, 35). A perforin-dependent, but Fas/FasL- and tumor necrosis factor alpha-independent, mechanism controls JHMV replication in astrocytes, microglia, and infiltrating macrophages (16, 22, 33). In perforin-deficient (PKO) mice, infectious virus clearance is delayed compared to in wild-type (wt) mice, resulting in survival of the host (16). In contrast, IFN- γ -deficient (GKO) mice exhibit increased mortality concomitant with compromised clearance of infectious virus from the CNS (21). In the absence of IFN- γ , virus replication is controlled in all cell types except oligodendrocytes, the cells which synthesize and maintain myelin, resulting in increased demyelination (21). These data are consistent with uncontrolled JHMV replication in all major CNS cell types in mice deficient in both perforin and IFN- γ (PKO/GKO mice), despite the efficient recruitment of CD4⁺ and CD8⁺ T cells to the CNS (5). The extent of myelin loss was decreased, but not absent, in infected PKO/GKO mice compared to wt mice. The

* Corresponding author. Mailing address: Keck School of Medicine, University of Southern California, 1333 San Pablo St., MCH 142, Los Angeles, CA 90033. Phone: (323) 442-1063. Fax: (323) 225-2369. E-mail: stohlman@hsc.usc.edu.

† Present address: Department of Microbiology, Universidad del Valle, Cali, Colombia.

‡ Present address: Laboratory of Immunoregulation, National Institutes of Health, Bethesda, Md.

adoptive transfer of memory CD8⁺ T cells from immune wt, GKO, or PKO mice into JHMV-infected PKO/GKO recipients demonstrated that CD8⁺ T cells control virus replication and prevent mortality, but at the cost of increased myelin loss (5). Demyelination increased to approximately the wt level in infected PKO/GKO recipients of wt or GKO memory CD8⁺ T cells. The distinct protective roles of perforin in controlling JHMV replication in astrocytes and IFN- γ in controlling oligodendroglia infection suggested that these effector mechanisms act in concert to mediate optimal viral clearance from the CNS in the presence of an otherwise intact endogenous inflammatory response (5).

The expression of antiviral effector functions *in vivo*, however, may be influenced by the host environment, *i.e.*, the presence of CD4⁺ T cells, or the CD8⁺-T-cell activation state. This is suggested by the differential ability of distinct JHMV-specific CD8⁺-T-cell populations to control viral replication and tissue damage. In contrast to the potent antiviral activity of nucleocapsid (N)-specific memory CD8⁺ T cells in infected BALB/c PKO/GKO recipients (5), activated viral spike (S) protein-specific CD8⁺ T cells exhibited weak antiviral activity in immunodeficient C57BL/6 Rag1^{-/-} recipients (23, 42). In the latter model, activated CD8⁺ T cells nonetheless contributed to demyelination in an IFN- γ -dependent manner (23). Previous results indicated increased apoptosis and decreased antiviral functioning of CD8⁺ T cells within the CNS in the absence of CD4⁺ T cells (34). In this report, the ability of memory CD8⁺ T cells to enter the JHMV-infected CNS, control virus replication, and induce CNS pathology in the absence of CD4⁺ T cells was examined via adoptive transfer of purified CD8⁺ T cells into infected SCID mice. Infected SCID mice were unable to control JHMV replication, lacked CNS inflammation, and showed no evidence of myelin loss, despite high levels of virus replication in oligodendroglia. JHMV-specific memory CD8⁺ T cells from wt donors reduced virus replication in all CNS cell types and initiated demyelination. CD8⁺ T cells derived from both PKO and GKO donors also entered the CNS and controlled JHMV replication. However, whereas PKO CD8⁺ T cells capable of IFN- γ secretion controlled virus replication in oligodendroglia, but not astrocytes, GKO CD8⁺ T cells capable of perforin-mediated cytotoxicity (19) controlled virus replication in astrocytes, but not oligodendroglia. In contrast to cells derived from wt donors, neither GKO nor PKO CD8⁺ T cells initiated demyelination in the absence of CD4⁺ T cells. Although the presence of IFN- γ -competent CD8⁺ T cells correlated with an increased infiltration of MHC class II-expressing macrophages, the degree of demyelination appeared independent of IFN- γ . These data support the concept that even in the absence of CD4⁺ T cells, CD8⁺ T cells utilize two separate effector mechanisms, cytotoxicity to control replication in astrocytes and IFN- γ secretion to control replication in oligodendroglia, to regulate virus replication within the CNS in a cell-type-dependent manner.

MATERIALS AND METHODS

Mice. SCID and syngeneic BALB/c (H-2^d) wt mice were obtained from the National Cancer Institute (Frederick, Md.) when they were 6 weeks old. Homozygous GKO BALB/c mice at the 7th backcross generation were provided by Robert Coffman (DNAX Research Corporation, Palo Alto, Calif.). Homozygous PKO BALB/c mice were generated in our laboratory as previously described (5)

and were used at the 11th backcross generation. Both GKO and PKO mice were maintained by intercrossing and were used at 6 to 7 weeks of age. SCID, GKO, and PKO mice were all maintained under sterile conditions.

Virus. The neutralizing monoclonal antibody (MAb)-derived 2.2v-1 variant of JHMV (8) was used for infections. The virus was propagated in the presence of MAb J.2.2 (8) and was plaque assayed on monolayers of DBT cells as previously described (8). Mice were injected in the left hemisphere with a 30- μ l volume containing 500 PFU of JHMV diluted in endotoxin-free Dulbecco's modified phosphate-buffered saline (PBS). For determination of CNS virus titers, one-half of the brains were homogenized on ice in Dulbecco's PBS by use of Tenbroeck tissue homogenizers. Following clarification by centrifugation at 500 \times g for 7 min, homogenates were stored at -70°C and virus titers were determined by plaque assays on monolayers of DBT cells, as previously described (3-5). Clinical disease was graded as previously described (8), with grades as follows: 0, healthy; 1, hunched back; 2, partial hind limb paralysis or inability to maintain upright position; 3, complete hind limb paralysis; 4, moribund or dead.

T-cell purification and adoptive transfer. BALB/c wt, GKO, and PKO donors were immunized by intraperitoneal injection with 1×10^6 to 2×10^6 PFU of JHMV. Donor cells were prepared from spleens at 4 to 16 weeks postimmunization. Spleen cells were depleted of B cells by adsorption onto 150-mm-diameter plates coated with goat anti-mouse immunoglobulin (ICN Pharmaceuticals, Costa Mesa, Calif.) or by adsorption to Immunolon columns (Biotex Laboratories, Houston, Tex.). CD8⁺ T cells were purified by either positive or negative selection. Briefly, for negative selection, CD4⁺ T cells and residual B cells were depleted with magnetic beads coated with anti-CD4 and anti-CD19 (Miltenyi Biotec Inc., Auburn, Calif.) antibodies according to the manufacturer's instructions. Alternatively, following the removal of B cells, CD8⁺ T cells were purified by positive selection with anti-Lyt2-coated magnetic beads (Miltenyi Biotec). Purity was assessed by flow cytometry using phycoerythrin (PE)-labeled anti-CD8⁺ (clone 53-6.7), fluorescein isothiocyanate (FITC)-labeled anti-CD4 (clone GK1.5), and FITC-labeled anti-CD19 (clone 1D3) (BD PharMingen, San Diego, Calif.) antibodies. CD8⁺ T cells were enriched to >96% by both approaches, and no differences in antiviral effector function were detected. CD8⁺ T cells specific for the immunodominant N epitope ranged from 5 to 15% of the total CD8⁺ T cells, as determined by flow cytometry using FITC-labeled anti-CD8 antibody and a PE-labeled L^d MHC class I tetramer associated with the pN318-326 peptide (L^dN318; 0.1 to 0.2 μ g/0.5 $\times 10^6$ to 1.0 $\times 10^6$ cells) (3). Recipients received 5×10^6 purified donor CD8⁺ T cells per mouse by intravenous injection 24 h prior to viral challenge.

CMCs. CNS-derived mononuclear cells (CMCs) were isolated from mice perfused with PBS by homogenization on ice with Tenbroeck tissue homogenizers as described above. Briefly, following centrifugation to obtain clarified homogenates for virus titer determination, cell pellets were suspended in RPMI medium containing 25 mM HEPES, pH 7.2, and adjusted to 30% Percoll (Pharmacia, Uppsala, Sweden). A 1.0-ml underlay of 70% Percoll was added prior to centrifugation at 800 \times g for 20 min at 4°C. Cells were recovered from the 30%-70% interface and washed in RPMI medium prior to analysis.

Flow cytometry. CMC suspensions were blocked with anti-mouse CD16/CD32 (clone 2.4G2; BD PharMingen) antibody on ice for 15 min prior to staining. For three-color flow cytometric analysis, cells were stained with FITC-, PE-, and CyC-conjugated MAbs at 4°C for 30 min in PBS containing 0.1% bovine serum albumin. Where indicated, four-color analysis was conducted using FITC-, PE-, allophycocyanin (PerCP)-, and peridinin chlorophyll protein (APC)-conjugated MAbs. The expression of surface molecules was characterized by using the following MAbs (all obtained from BD PharMingen except where indicated): anti-CD8 (clone 53-6.7), anti-CD4 (clone GK1.5), anti-CD19 (clone 1D3), and anti-pan-NK (clone DX5). Neutrophils were identified with anti-Ly-6G/6C MAb (clone RB6-8C5). Virus-specific CD8⁺ T cells were detected by staining with FITC-labeled anti-CD8 antibody and PE-labeled L^dN318 tetramers. PE- or CyC-conjugated anti-CD45 (Ly-5) and anti-F4/80 (Serotec, Raleigh, N.C.) antibodies, or in some experiments, anti-CD11b (M1/70) antibody, distinguished microglia (CD45^{lo} F4/80⁺; CD45^{lo} CD11b⁺) from infiltrating or perivascular macrophages (CD45^{hi} F4/80⁺; CD45^{hi} CD11b⁺). MHC expression on microglia was determined by using an anti-H-2 D^d-specific MAb (clone 34-2-12), anti-I-A/I-E MAb (clone 2G9), or anti-I-A^d MAb (clone 39-10-8). Due to the consistent reactivity of the anti-F4/80 MAb with a subset of Ly-6G/6C⁺ cells, neutrophils were characterized as Ly-6G/6C⁺ class II⁻, whereas infiltrating macrophages were defined as F4/80⁺ class II⁺. Samples were analyzed on a FACStar or FACSCalibur flow cytometer (Becton Dickinson, Mountain View, Calif.). Forward and side scatter signals obtained in linear mode were used to establish a region (R1) containing live lymphocytes, macrophages, and neutrophils, while excluding dead cells and tissue debris. A minimum of 2.5×10^5 viable cells were stained and 5×10^4 to 1×10^5 events were analyzed per sample.

Histopathological analysis. Brains and spinal cords were removed and either fixed with Clark's solution (75% ethanol and 25% glacial acetic acid) and embedded in paraffin or snap frozen. Paraffin sections were stained with either hematoxylin and eosin or luxol fast blue. For identification of virus antigen-positive cells, mice were perfused with 4% paraformaldehyde in PBS (pH 7.4). Brains and spinal cords were removed, postfixed with 4% paraformaldehyde at 4°C for 24 h, and then equilibrated with 30% sucrose in PBS (pH 7.4) by overnight incubation at 4°C. Frozen sections were stained with MAb J.3.3, specific for the viral N protein, and a MAb specific for astrocytes (glial fibrillary acidic protein; Dako, Carpinteria, Calif.) or macrophages (F4/80; SeroTec), as previously described (3–5, 16, 17). JHMV antigen and glial fibrillary acidic protein double staining was visualized with peroxidase Vector VIP and Vector SG substrate kits (both from Vector Laboratories, Burlingame, Calif.), respectively. Viral antigen in F4/80-positive cells was detected with an alkaline phosphatase Vectastain ABC kit for MAb J.3.3 and a peroxidase Vectastain ABC kit with AEC substrate (both from Vector Laboratories) for MAb F4/80.

CD8⁺ and CD4⁺-T-cell infiltration was examined by immunoperoxidase staining of acetone-fixed frozen sections with rat anti-CD8a (Ly-2) and anti-CD4 (L3T4) MAbs (BD PharMingen) as previously described (14, 15). Primary MAbs were detected by immunoperoxidase staining with a biotinylated rabbit anti-rat antibody (Vector Laboratory) and a Vectastain ABC kit. Aminoethyl carbazol was used as the chromogen substrate (Vector Laboratories). Apoptotic cells were identified in acetone-fixed frozen sections by a terminal deoxynucleotidyltransferase-mediated dUTP-biotin nick end labeling assay using an Apop Tag kit (Oncor, Gaithersburg, Md.) with terminal deoxynucleotidyltransferase, as indicated by the manufacturer. Sections were scored in a blinded fashion for inflammation, viral antigen, and demyelination. Representative fields were identified based on average scores for all sections in each experimental group.

RESULTS

JHMV pathogenesis in immunodeficient SCID mice. CD8⁺ T cells play a major role in the control of JHMV replication within the CNS via IFN- γ secretion and perforin-mediated cytolysis (5, 16, 21). Nevertheless, CD4⁺ T cells contribute to JHMV-specific CD8⁺ T cell expansion and survival within the CNS (34), in addition to being potent sources of IFN- γ secretion themselves (30). For evaluation of antiviral effector functions as well as the pathogenic potential of memory CD8⁺ T cells in the absence of CD4⁺ T cells, JHMV pathogenesis was analyzed in immunodeficient SCID mice. For initial confirmation of the importance of adaptive immunity in controlling JHMV infections (3, 4, 12, 15, 40), SCID mice were compared to wt mice. In infected wt mice, JHMV replication in the CNS peaked at 5 days postinfection (p.i.), declined beginning at day 7 p.i., and was below the level of detection by day 14 p.i. (Fig. 1). No clinical disease was detected in infected wt or SCID mice prior to day 10 p.i. Beginning at day 10 p.i., wt mice exhibited clinical evidence of encephalomyelitis which increased dramatically with time, consistent with previous data (8, 17, 21, 25). SCID mice exhibited barely detectable clinical disease throughout the infection, with a minimal average clinical score of ≤ 1.0 . The majority of infected SCID mice succumbed between days 15 and 18 p.i., with vary rare individuals surviving until 22 days p.i. The unchecked JHMV replication from days 5 to 14 p.i. in infected SCID mice contrasts with the immune-mediated control of infectious virus from days 7 to 14 p.i. in wt mice (Fig. 1) and the partial control of virus in the CNS of mice deficient in the expression of IFN- γ , perforin, or both effectors (5, 16, 21). The absence of clinical disease in infected SCID mice is consistent with the suggestion that inflammatory responses contribute to clinically evident neurological symptoms (12, 13, 24).

A comparison of the pathological consequences of infection in the absence of adaptive immunity showed an absence of

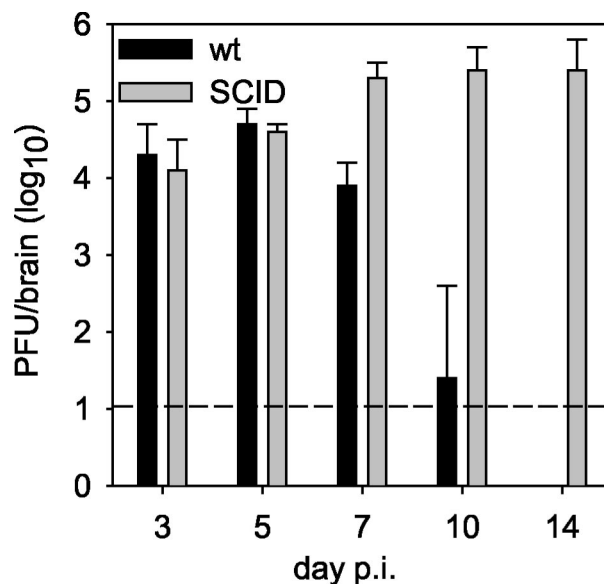


FIG. 1. JHMV replication in the CNS of SCID and wt mice. SCID and syngeneic wt BALB/c control mice were infected with 500 PFU of JHMV. Mice were sacrificed at various times p.i. and JHMV replication in the CNS was examined by plaque assays of brain homogenates. Each point is the average for three to five mice per group, and the data are representative of three separate experiments.

inflammation in the CNS of infected SCID mice, in contrast to a vigorous inflammatory response in wt mice (Fig. 2). The viral antigen level was dramatically higher in the CNS of SCID mice after day 3 p.i. and was abundant in all CNS cell types, including astrocytes, oligodendroglia, microglia/macrophages (Fig. 2A), and even occasional neurons (data not shown), at day 14 p.i. In contrast, only scattered cells positive for viral antigen, for which the level had dramatically decreased from the levels found during acute infection, were detected in the brains of infected wt mice at day 14 p.i. (Fig. 2B). Similarly, the viral antigen level was also dramatically increased in spinal cords of infected SCID mice relative to those of wt mice, and the antigen was present in all cell types in both gray and white matter, although more virus-infected cells were detected in the white matter than in the gray matter (Fig. 2C). In contrast to wt mice, occasional neurons were infected in the spinal cords of SCID mice, although the numbers did not increase in the rare survivors up to day 21 p.i. (data not shown). In spinal cords of wt mice, the residual viral antigen level decreased relative to the levels found during acute infections, and antigen was localized predominantly in white matter cells exhibiting morphological characteristics consistent with oligodendroglia (Fig. 2D). Coincident with viral clearance, demyelination in wt mice was apparent as early as day 10 p.i. (4, 8, 15, 25; data not shown). However, despite numerous infected oligodendroglia in the spinal cords of infected SCID mice, demyelination was absent from both the brains and spinal cords at day 14 p.i. (Fig. 2E and F). However, in contrast to the case for immunodeficient Rag1^{-/-} mice, which also show no myelin loss following JHMV infection (23, 24, 42), occasional small foci of demyelination were found in the spinal cords of the rare infected SCID mice which survived to later time points (data not shown).

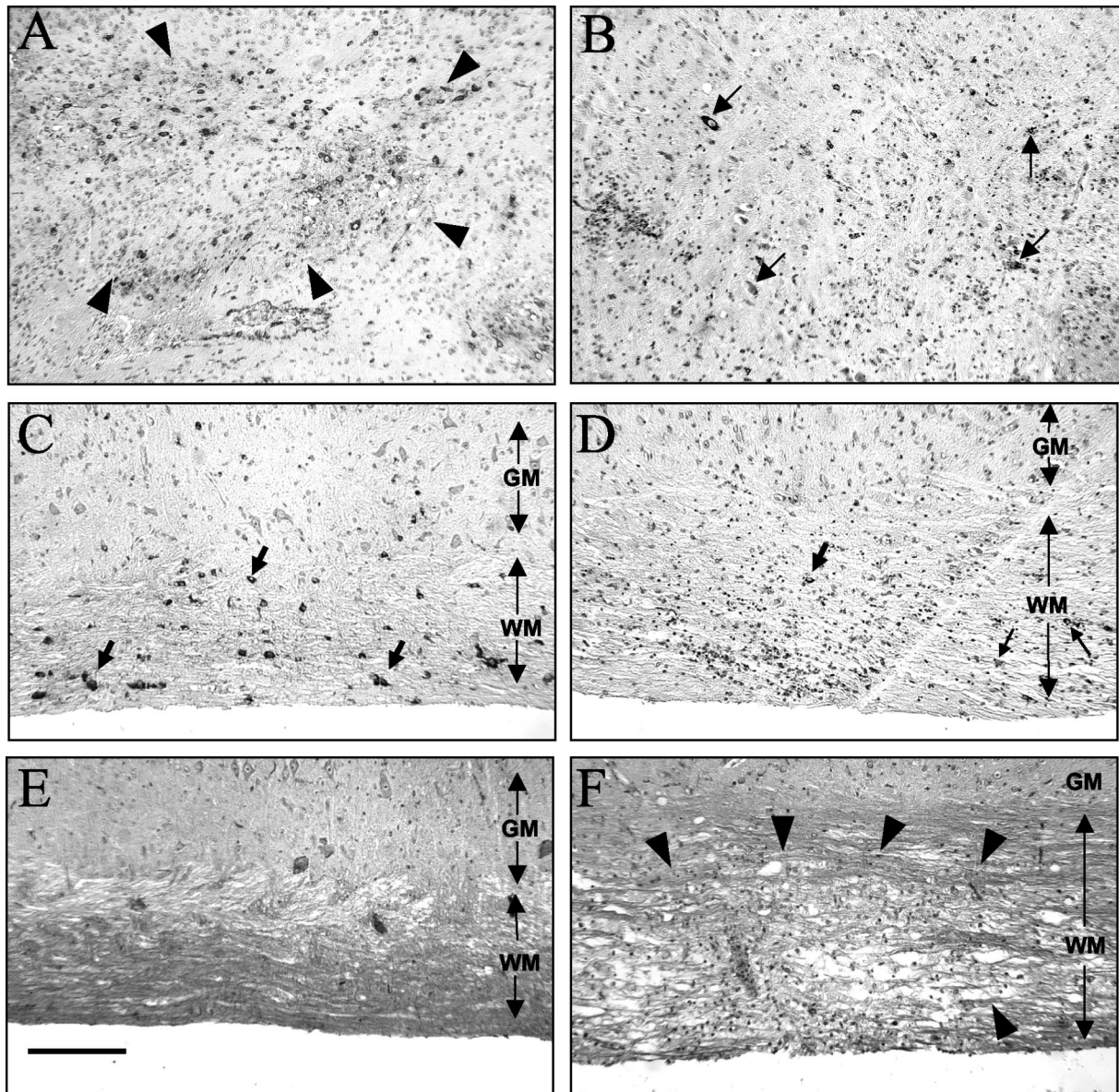


FIG. 2. Pathological changes in the CNS of SCID versus wt mice infected with JHMV. JHMV antigen and inflammation in the brains of JHMV-infected SCID (A) and wt (B) mice at day 14 p.i. (immunoperoxidase stain for JHMV antigen, with hematoxylin counterstain) are shown. (A) The area outlined by arrowheads contains numerous antigen-positive cells. (B) Only rare antigen-positive cells are seen (arrows). JHMV antigen and inflammation in the spinal cords of JHMV-infected SCID (C) and wt (D) mice are also shown. The extent of the white matter (WM) and gray matter (GM) is indicated by double-headed arrows. (C) Numerous antigen-positive cells are seen in the white matter (arrows). (D) Only very rare antigen-positive cells are seen in the white matter (arrow). (E and F) Luxol fast blue staining of spinal cord sections showed no demyelination in infected SCID mice (E) and large areas of demyelination (arrow heads) in infected wt mice (F). Bar = 50 μ m.

These small foci of myelin loss are consistent with the suggestion that oligodendroglial infection may contribute to focal demyelination (2, 12–15). Flow cytometric analysis of the cells derived from the CNS of infected SCID mice at day 10 p.i. showed $\sim 30\%$ CD45^{hi} infiltrating cells, of which the vast majority (60 to 70%) were neutrophils, with 10% and 5 to 8% constituting NK cells and macrophages, respectively. By this time, infected wt mice had only $\sim 7\%$ neutrophils and 2% NK cells in the CD45^{hi} population. Macrophages constituted $\sim 25\%$, while T cells comprised a predominant 65%, as previously described (5, 23; data not shown).

Antiviral CD8⁺-T-cell effector function within the CNS. JHMV replication is inhibited via both IFN- γ secretion and perforin-mediated cytotoxicity. Although CD8⁺ T cells exert these antiviral activities, their functioning is partially dependent upon CD4⁺ T cells (34). For evaluation of the sole antiviral functions of CD8⁺ T cells and dissection of the relative contributions of IFN- γ and perforin-mediated cytolysis in the absence of CD4⁺-T-cell-mediated help, CD8⁺ T cells derived from immunized wt, PKO, and GKO donors were adoptively transferred into SCID recipients. Although CD8⁺ T cells activated *in vitro* or obtained from actively infected donors traffic

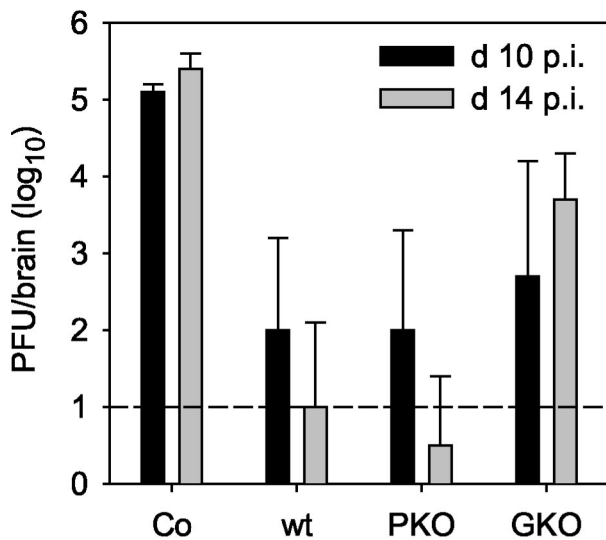


FIG. 3. Memory CD8⁺ T cells suppress JHMV replication within the CNS. JHMV replication was analyzed at days 10 and 14 p.i. in the CNS of untreated JHMV-infected SCID mice (Co) and recipients of 5×10^6 purified CD8⁺ T cells derived from JHMV-immune wt, PKO, and GKO donors. Data represent the averages of three to six mice per group and are representative of three or four separate experiments.

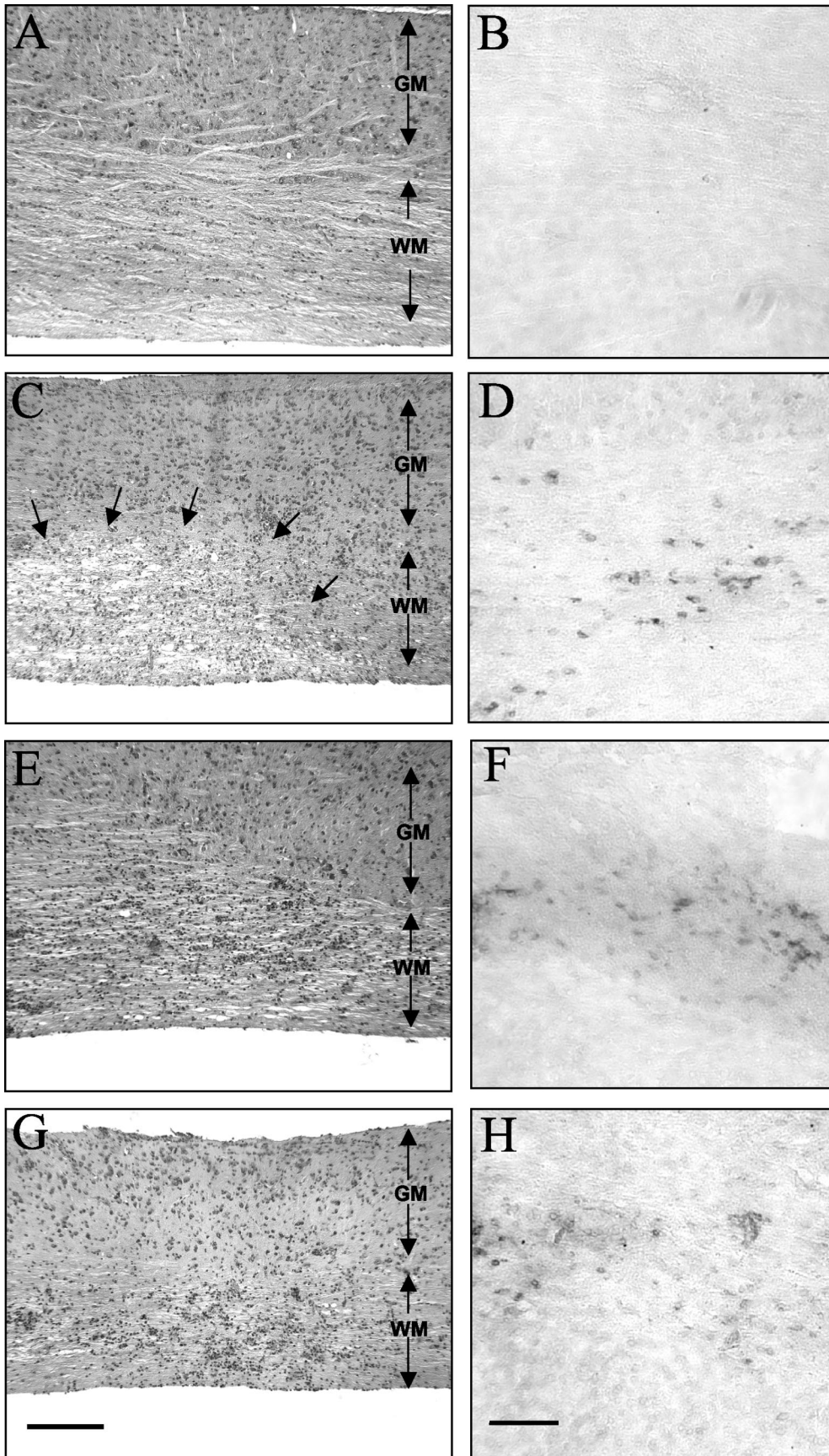
into the JHMV-infected CNS (32, 34, 36), memory populations were chosen to diminish the loss of activated T cells in the liver and potential activation-induced cell death within the infected CNS (28). Antiviral functioning was assessed by comparing viral replication within the CNS of infected SCID mice and those of infected SCID CD8⁺-T-cell recipients. CD8⁺ T cells derived from wt donors reduced virus replication in the CNS of SCID recipients at day 10 p.i. compared to untreated controls and continued to be effective at controlling infectious virus to near the limits of detection to day 14 p.i. (Fig. 3). These data demonstrate that CD8⁺ T cells are recruited into the JHMV-infected CNS in the absence of CD4⁺ T cells and that they express effective antiviral functions. No evidence for antiviral activity was detected in the CNS at day 10 p.i. following the adoptive transfer of purified CD8⁺ T cells from naïve donors into SCID recipients, and only a small effect (<1 log₁₀ reduction) was detected at day 14 p.i. (data not shown). The results confirmed that antiviral effects reside in the virus-specific memory CD8⁺ T cells rather than in primed naïve CD8⁺ T cells contained within the transferred population.

The relative contribution of a perforin-dependent mechanism for controlling JHMV replication in the absence of IFN- γ was examined by the transfer of CD8⁺ T cells derived from immunized GKO donors. GKO CD8⁺ T cells were less efficient at controlling viral replication than were wt CD8⁺ T cells at day 10 p.i. (Fig. 3), and their impaired antiviral function was even more apparent by day 14 p.i. (Fig. 3). The inability of GKO CD8⁺ T cells to sustain control of viral replication was confirmed after the transfer of in vitro-activated CD8⁺ T cells (data not shown). The reduced ability of GKO CD8⁺ T cells to control virus replication in SCID recipients is consistent with results for transfer into PKO/GKO recipients (5) and the in-

ability of infected GKO mice to clear infectious virus from the CNS (21).

CD8⁺ T cells from PKO donors that are competent in IFN- γ secretion but unable to mediate cytolysis were approximately as efficient as CD8⁺ T cells derived from both wt and GKO donors at controlling viral replication within the CNS at day 10 p.i. (Fig. 3). However, in contrast to GKO CD8⁺ T cells, PKO CD8⁺ T cells suppressed viral replication to similar levels as the wt donor cells did at 14 days p.i. (Fig. 3). The ability of PKO CD8⁺ T cells to control JHMV replication within the CNS is consistent with the delayed, but complete, clearance of JHMV from the CNS of infected PKO mice (16) but contrasts with the less effective virus control following transfer into PKO/GKO hosts containing CD4⁺ T cells (5). This apparent dichotomy may be due to homeostatic parameters resulting in enhanced expansion and CNS recruitment of donor T cells in SCID mice compared to spatial constraints in PKO/GKO hosts. Cells derived from the CNS of infected SCID recipients of both wt and GKO donors exhibited ex vivo JHMV-specific cytotoxic activity at day 7 p.i. (data not shown). In addition, cells derived from the CNS of infected SCID recipients of both wt and PKO CD8⁺ T cells secreted IFN- γ following in vitro stimulation (data not shown). The ability to express cytolytic activity, secrete IFN- γ , and importantly, control CNS virus replication demonstrates that memory CD8⁺ T cells exert functional activity within the CNS of infected SCID recipients even in the absence of CD4⁺-T-cell support.

Altered CNS inflammation in the presence of donor CD8⁺ T cells. Inflammatory responses were compared in the CNS of infected SCID mice and infected SCID CD8⁺-T-cell recipients by immunohistochemistry at day 14 p.i. to assess the degree of inflammation as well as the distribution of CD8⁺ T cells. No inflammatory cells or CD8⁺ T cells were detected in the CNS of infected SCID mice (Fig. 4A and B). In contrast, wt CD8⁺ T cells induced vigorous inflammatory responses in both brains and spinal cords (Fig. 4C and D). CD8⁺ T cells from wt donors were present in the brain parenchyma and the white matter of the spinal cord (Fig. 4D), consistent with the reduced infectious virus level (Fig. 3). In contrast to unmanipulated infected SCID mice, no infected neurons were noted in recipients of wt CD8⁺ T cells. CD8⁺ T cells deficient in either IFN- γ or perforin also induced vigorous CNS inflammation (Fig. 4E to H) and were distributed within the brain parenchyma and the spinal cord white matter, similar to those derived from wt donors. Less efficient control of virus replication (Fig. 3) could thus not be attributed to impaired tissue access. An increased frequency of apoptotic cells with the morphology of lymphocytes was detected within the parenchyma of both wt and PKO CD8⁺-T-cell recipients compared to untreated infected SCID mice. However, reduced numbers of apoptotic cells were detected in the CNS of GKO T-cell recipients (data not shown), consistent with the notion that IFN- γ diminishes CD8⁺-T-cell survival (1). Overall, these data support the concept that CD8⁺ T cells entering the infected CNS in the absence of CD4⁺ T cells exhibit an increased frequency of apoptosis (32). CD8⁺ T cells derived from wt donors induced demyelination in the CNS of infected SCID recipients (Fig. 4C), similar to infected wt mice (Fig. 2) and PKO/GKO recipients of wt CD8⁺ T cells (5). However, inflammation by GKO or PKO CD8⁺ T cells did not induce myelin loss in SCID recipients (Fig. 4E and G). The



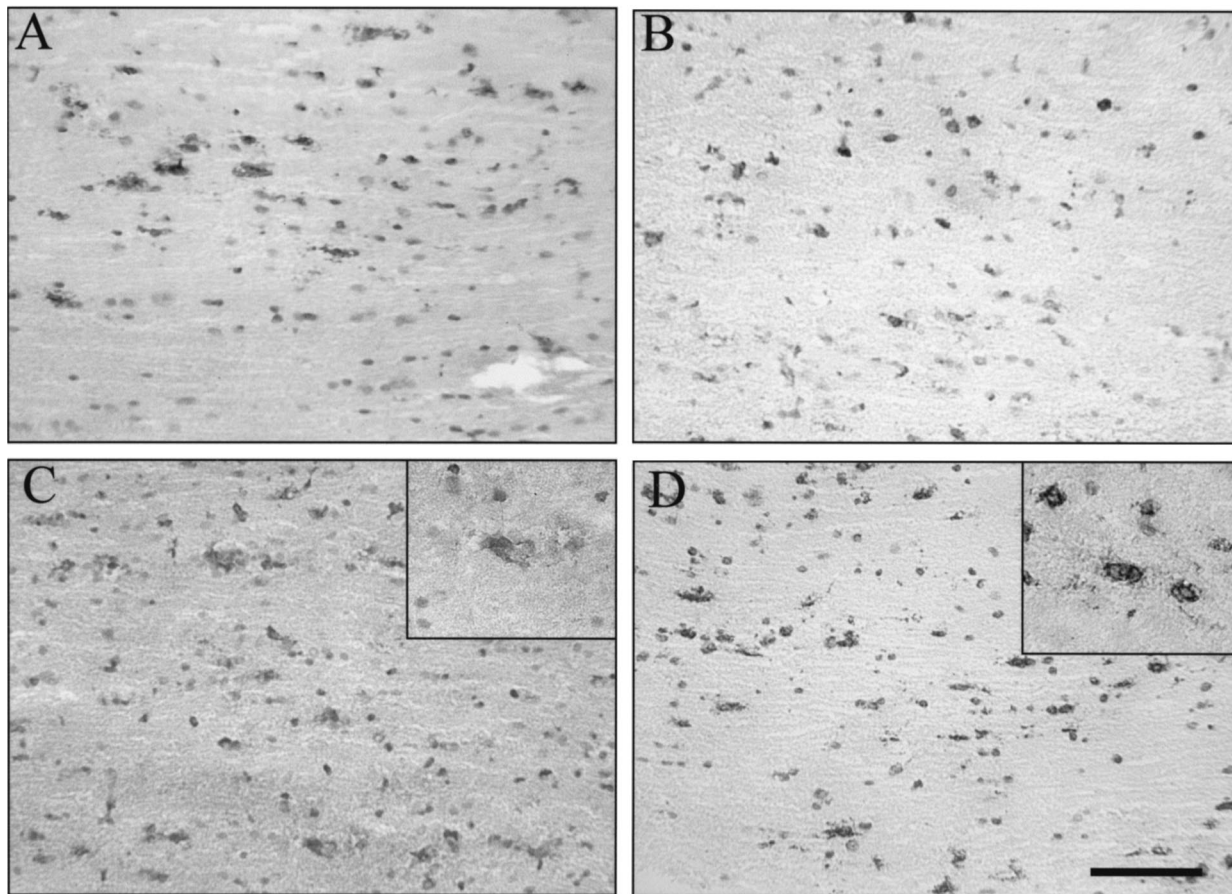


FIG. 5. Viral antigen distribution in brains of JHMV-infected SCID mice reconstituted with CD8⁺ T cells. Brain sections from infected SCID mice at 10 days p.i. show numerous antigen-positive astrocytes and oligodendroglia in the white matter (A). Infected SCID recipients of memory CD8⁺ T cells derived from wt donors show fewer antigen-positive cells (B). Infected SCID recipients of PKO-derived CD8⁺ T cells (C) show many antigen-positive astrocytes (inset), but very few antigen-positive oligodendroglia. Infected SCID recipients of GKO-derived CD8⁺ T cells (D) show many antigen-positive oligodendroglia (inset), but very few antigen-positive astrocytes. Panels were stained for viral antigen with immunoperoxidase, with a hematoxylin counterstain. Bar = 100 μ m.

predominant localization of all three populations of CD8⁺ T cells within the spinal cord white matter (Fig. 4F and H) supports the notion that demyelination is not associated with the presence of CD8⁺ T cells capable of either IFN- γ or perforin secretion alone.

Differential susceptibility of glial cells to CD8⁺-T-cell-mediated effector mechanisms. An analysis of JHMV infection in PKO/GKO recipients of virus-immune CD8⁺ T cells (5) supported the concept that perforin-mediated cytotoxicity controls virus replication in astrocytes and macrophages/microglia while IFN- γ controls virus replication in oligodendroglia (16,

21). The CNS of infected SCID recipients were examined to determine if donor CD8⁺ T cells alone, in the absence of other potential adaptive antiviral immune effectors, specifically CD4⁺ T cells, regulated virus replication in specific CNS cell types via distinct effector mechanisms. In infected SCID mice, the viral antigen was prominent in both astrocytes and oligodendroglia, with approximately equal numbers of infected cells (Fig. 2 and 5). Concomitant with a reduction in recoverable infectious virus in recipients of wt CD8⁺ T cells (Fig. 3 and 4), an ~70% reduction in virus-infected astrocytes and oligodendroglia was observed compared to untreated SCID mice (Fig.

FIG. 4. Inflammation and CD8⁺-T-cell distribution in spinal cords of JHMV-infected SCID mice reconstituted with CD8⁺ T cells at day 14 p.i. The extent of the spinal cord white matter (WM) and gray matter (GM) is indicated by double-headed arrows. Sections of infected SCID mice show no inflammatory infiltrates (A) or CD8⁺ T cells (B). Infected SCID mice that are recipients of 5×10^6 purified memory CD8⁺ T cells derived from wt donors show prominent demyelination (outlined by arrows) (C) and CD8⁺-T-cell infiltrates in the white matter (D). Infected SCID mice that are recipients of CD8⁺ T cells derived from GKO donors show white matter inflammation (E) and CD8⁺-T-cell infiltrates (F). Infected SCID mice that are recipients of CD8⁺ T cells derived from PKO donors show white matter inflammation (G) and CD8⁺-T-cell infiltrates (H). Panels A, C, E, and G were stained with hematoxylin and eosin. Bar = 200 μ m. Panels B, D, F, and H were stained for CD8⁺ T cells with immunoperoxidase. Bar = 100 μ m.

5B). Similar to wt donor CD8⁺ T cells, GKO CD8⁺ T cells reduced the number of infected astrocytes in spinal cords (Fig. 5D). However, no reduction was found in infected oligodendroglia compared to the case for untreated SCID mice. In contrast, in SCID recipients of PKO CD8⁺ T cells the number of infected astrocytes was comparable to that in untreated SCID mice; however, the frequency of infected oligodendroglia was dramatically reduced (Fig. 5C). Despite suppressed virus replication (Fig. 3) and reduced infected oligodendroglia, rare infected neurons were detected in PKO CD8⁺-T-cell recipients, in contrast to SCID recipients of either wt or GKO CD8⁺ T cells. Although few infected F4/80⁺ cells were detected in the CNS of any recipient group compared to wt mice, the overall distribution of F4/80⁺ cells in the CNS was similar. The low frequency of this population, as detected by immunohistochemistry (data not shown), precluded determination of the effects of IFN- γ and perforin-mediated cytolysis on virus replication in this cell type. These data are nevertheless consistent with the inability of perforin-mediated cytolysis to control JHMV replication in oligodendroglia and the inability of infected PKO mice to inhibit virus replication in astrocytes, as previously observed with CD4-competent mice (5, 16).

For a more quantitative determination of subsets of inflammatory cells, CNS-derived cells from infected SCID mice and all three recipient groups were analyzed by flow cytometry (Fig. 6). Compared to those for infected control SCID mice, CNS yields were consistently higher for recipient groups, but varied in absolute numbers between experiments. In the CNS of infected untreated SCID mice, CD45^{hi} bone-marrow-derived inflammatory cells comprised ~30% of the cells at day 10 p.i. (Fig. 6A). The majority of CD45^{hi} cells were Ly-6G/6C⁺ and MHC class II⁻, consistent with the case for neutrophils (Fig. 6B). NK cells and MHC class II⁺ F4/80⁺ macrophages each comprised <10% of the infiltrating cells (Fig. 6B). No CD4⁺ or CD8⁺ T cells were detected in the CNS of infected control SCID mice. CD45^{hi} cells derived from the CNS cells of all CD8⁺-T-cell recipient groups ranged from 25 to 40% (Fig. 6A). However, these populations contained significantly reduced percentages of neutrophils and NK cells. These data suggest that CD8⁺ T cells, irrespective of the ability to secrete IFN- γ or perforin, reduce the accumulation and/or retention of neutrophils and NK cells. In contrast, relative to the levels detected in untreated SCID mice, the frequency of infiltrating CD45^{hi} MHC class II⁺ F4/80⁺ macrophages was elevated in recipients of IFN- γ -secreting CD8⁺ T cells (Fig. 6B). No increase in infiltrating macrophages was found in recipients of GKO CD8⁺ T cells, supporting the concept that CNS inflammation by CD8⁺ T cells able to secrete IFN- γ enhances the recruitment and/or retention of bone-marrow-derived macrophages (22, 39). Note the equivalent frequencies of macrophages recruited into the brains of recipients of both wt- and PKO-derived CD8⁺ memory T cells. Their frequency was even higher in spinal cords of wt and PKO CD8⁺-T-cell recipients, constituting up to 50% of infiltrating cells (data not shown). Nevertheless, demyelination was only present in the CNS of wt recipients, while no demyelination was detected in the CNS of recipients of PKO CD8⁺ T cells (Fig. 4 and 5).

Consistent with the control of virus replication and reduced viral antigen, 35 to 55% of the inflammatory cells recovered from the CNS of all recipients comprised CD8⁺ T cells (Fig.

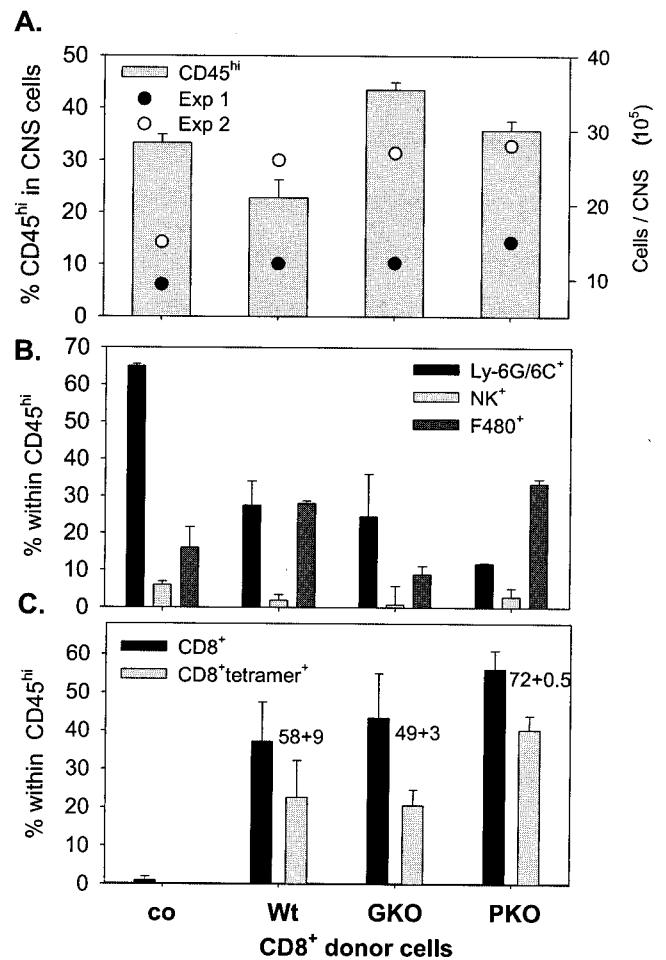


FIG. 6. Composition of CNS infiltrates following transfer of donor CD8⁺ T cells. Single-cell suspensions from brains were prepared from infected untreated SCID mice (co) or recipients of CD8⁺ T cells from wt, GKO, and PKO immune donors, as indicated, at 10 days p.i. ($n = 3$ to 4/group). CNS-derived cells were stained with anti-CD45, anti-Ly-6G/6C, anti-NK, anti-F4/80, anti-I-A/E^d, anti-CD8, L^d-N318 tetramer, and anti-CD4 antibodies and were analyzed by flow cytometry. All data depict average percentages \pm standard errors from two independent experiments. (A) Bars depict the percentages of infiltrating CD45^{hi} cells in total viable CMCs; the live gate R1 region typically comprised 40 to 50% of total events. Total yields of viable cells per CNS from two separate experiments ($n = 3$ or 4/group) are shown for reference. (B) Relative percentages of Ly-6G/6C⁺ class II⁻ neutrophils, NK cells, and class II⁺ F4/80⁺ macrophages within the infiltrating CD45^{hi} population. Data were calculated based on setting the CD45^{hi} population to 100%. (C) Relative percentages of total CD8⁺ and tetramer-positive CD8⁺ cells within the CD45^{hi} population. The numbers adjacent to the columns depict the relative percentages of tetramer-positive cells within the respective CD8⁺ populations. CD4⁺ T cells were barely detectable in the CD45^{hi} population (<4%) for all recipients. Data are representative for two additional experiments in which CMCs from brains and spinal cords were pooled.

6C). Virus-specific cells comprised >50% of the total CD8⁺ T cells within the CNS of both wt and GKO recipients. The frequencies of both total and virus-specific CD8⁺ T cells in CNS-derived CD45^{hi} cells from PKO recipients were consistently increased compared to those in recipients of wt- and GKO-derived CD8⁺ T cells, possibly reflecting the inhibitory

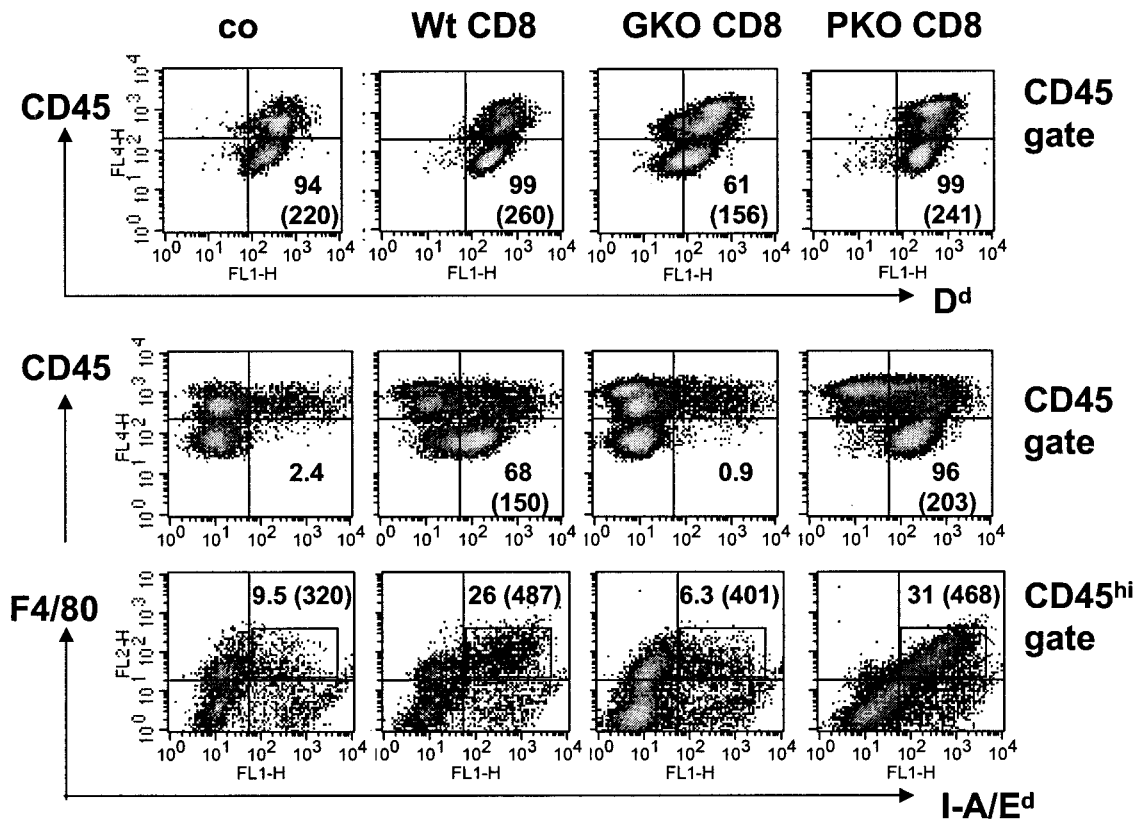


FIG. 7. MHC expression on microglia/macrophages following transfer of donor CD8⁺ T cells. Data are shown for single-cell brain suspensions from infected untreated SCID mice (co) or recipients of CD8⁺ T cells from wt, GKO, or PKO immune donors at 10 days p.i. (*n* = 3 or 4/group). Cells were stained with APC-conjugated anti-CD45 antibody and various combinations of PE-conjugated anti-F4/80, FITC-conjugated anti-class I D^d, and FITC-conjugated anti-class II I-A/E^d and were analyzed by flow cytometry. (Top and middle) Density plots gated on total CD45⁺ cells comprising both CD45^{lo} resident microglia and CD45^{hi} infiltrating cells. Quadrants were set to separate MHC-negative and -positive (*x* axis) microglia (CD45^{lo}) from infiltrating (CD45^{hi}) cells (*y* axis). Numbers represent percentages of class I D^{d+} or class II I-A/E^{d+} cells within the microglia population. Parentheses in the lower right quadrant indicate mean fluorescence intensities of class I⁺ or class II⁺ microglia. Class I and class II expression was undetectable on microglia in uninfected mice (data not shown). (Bottom) Density plots gated on CD45^{hi} cells comparing class II expression on infiltrating macrophages. The rectangle comprises class II⁺ F4/80⁺ infiltrating macrophages; numbers depict percentages within the CD45^{hi} population, as well as the mean fluorescence intensities of class II expression (in parentheses).

role of perforin on CD8⁺-T-cell expansion (1, 31). The increased frequency of virus-specific CD8⁺ T cells derived from PKO donors may also reflect ongoing stimulation by antigen-positive astrocytes, suggesting that continued expression of viral antigens may contribute to the magnitude and duration of CD8⁺-T-cell responses.

One possibility for ineffective CD8⁺-T-cell-mediated clearance is insufficient MHC upregulation on resident CNS cells, although NK cells, a potential source of IFN- γ , are present in the CNS of infected SCID mice. MHC expression was therefore compared on resident CD45^{lo} microglia from control and recipient mice at day 10 p.i. Microglia from naïve mice express few, if any, MHC class I molecules (5, 29). However, the majority of microglia in infected SCID mice expressed class I molecules, and transferred CD8⁺ T cells did not dramatically alter their expression (Fig. 7). IFN- γ -competent wt and PKO CD8⁺ T cells had slightly enhanced expression, while GKO donor cells had a reduced frequency as well as intensity of class I expression on microglia. Thus, the specific inability of cells from GKO donors to control JHMV infections could not be attributed to an absence of MHC class I expression on resident

CNS cells. In contrast to MHC class I, MHC class II expression was dramatically affected by IFN- γ secretion by donor CD8⁺ T cells. Class II molecule expression was undetectable on microglia in both infected control and GKO CD8⁺-T-cell recipients. In contrast, wt and PKO CD8⁺ T cells induced class II expression on 70 and 96% of microglia, respectively, thus providing direct *in vivo* evidence for IFN- γ secretion. In contrast to microglia, class II expression by infiltrating macrophages was higher in all groups of mice, with the highest expression detected in recipients of IFN- γ -competent donor T cells. The effects of IFN- γ were thus manifested by the enhanced overall recruitment of CD45^{hi} class II⁺ F4/80⁺ macrophages and class II induction on microglia, in addition to the reduction in virus load observed in PKO recipients.

DISCUSSION

The analysis of CD8⁺-T-cell antiviral mechanisms employed during acute JHMV-induced disease has provided insights into the inability of the immune system to control the establishment of viral persistence and chronic CNS demyelination (10, 13, 15,

18, 35). CD8⁺ T cells reduce viral replication via a combination of perforin-mediated cytolysis and IFN- γ secretion and protect the host from lethal disease (5, 16, 21, 22, 25, 36). Although cytolytic activity is rapidly lost as infectious virus is controlled (3, 18, 25), CD8⁺ T cells are retained within the CNS as long as viral antigen or viral RNA persists (19). CD4⁺ T cells play a supporting role in JHMV clearance from the CNS. They facilitate CD8⁺-T-cell expansion, localize primarily to the perivascular and subarachnoid spaces, and enhance the survival of parenchymal CD8⁺ T cells, but they also contribute to the severity of clinical signs associated with CNS infection (24, 34, 42). Memory CD8⁺ T cells transferred into PKO/GKO hosts with normal lymphoid compartments were effective at limiting CNS virus replication (5). However, a potential role of host CD4⁺-T-cell responses in the infected recipients was not excluded (5). The present experiments were undertaken to determine the potential of memory CD8⁺ T cells alone to limit virus replication as well as to support distinct antiviral roles of perforin-mediated cytolysis and IFN- γ within the CNS in the absence of CD4⁺ T cells.

JHMV replication was completely uncontrolled within the CNS of SCID mice, similar to both lethally irradiated and other types of immunodeficient mice (12, 23, 24, 40, 42, 44). The CNS infiltrate of untreated infected SCID mice was largely composed of neutrophils. Interestingly, this population was dramatically reduced during CD8⁺-T-cell infiltration, independent of perforin or IFN- γ . Neutrophils are among the first cell types to enter the CNS during an acute infection and contribute to the loss of vascular permeability, thereby facilitating inflammatory cell entry (44). However, the uncontrolled virus replication in the CNS of untreated SCID mice indicates limited, if any, direct antiviral activity. Furthermore, the analysis of JHMV pathogenesis in SCID mice confirmed previous data suggesting that NK cells lack the ability to directly control virus replication in the CNS (12, 23, 24, 42). The possible antiviral role for NK cells implicated by the analysis of mice depleted of either CD4⁺ T cells or CD8⁺ T cells (12, 40) may thus involve an indirect effect exerted on antigen presentation.

CD8⁺ memory T cells from wt donors reduced JHMV replication at both 10 and 14 days p.i., consistent with the concept that CD8⁺ T cells are primary effectors of virus clearance (13, 15, 18). Nevertheless, in contrast to the long-term survival of PKO/GKO recipients of wt cells, all SCID recipients were unable to completely clear infectious virus and eventually succumbed to JHMV infection (data not shown). In vitro-activated memory cells also controlled virus replication in the CNS of SCID recipients (data not shown), suggesting that resting or reactivated memory CD8⁺ T cells exhibit a similar protective capacity in this system. Whether the differential abilities of donor CD8⁺ T cells to control virus replication in SCID versus Rag1^{-/-} recipients (23, 42) reside in the distinct activation statuses of the donor cells or the different immunodominant epitopes recognized remains unresolved. One explanation may be that BALB/c donor T cells respond dominantly to a conserved epitope in the N protein, while H-2^b CD8⁺ T cells transferred to Rag1^{-/-} recipients mount dominant responses to a more variable epitope in the viral S protein, enhancing the likelihood for cytotoxic T-lymphocyte escape mutations. Nevertheless, together these data suggest that both highly activated and memory CD8⁺ T cells access the CNS in the absence of

CD4⁺ T cells and initiate the process that ultimately results in demyelination (23, 42).

The ability of PKO CD8⁺ T cells to control virus replication supports the concept that IFN- γ is critical for antiviral activity (5, 21). Furthermore, an analysis of the CNS of JHMV-infected PKO mice, as well as PKO/GKO recipients of PKO CD8⁺ T cells, indicated that in the absence of perforin, virus replication was controlled in oligodendroglia, but not in astrocytes and macrophages/microglia. Although it is not clear if astrocytes express MHC class I molecules during JHMV infection (26), perforin-dependent control of JHMV replication implicates the recognition of antigens in the context of MHC class I. A comparison of the CNS of JHMV-infected SCID mice and SCID recipients of PKO CD8⁺ T cells confirmed that CD8⁺ T cells have a limited ability to control virus replication in astrocytes in the absence of perforin-mediated cytolysis (16). The participation of perforin in the control of virus replication in myelomonocytic lineage cells could not be determined due to the paucity of cells from this lineage in the CNS of infected SCID mice. However, it is interesting that CD8⁺ T cells from wt and GKO donors prevented the rare infection of neurons noted in untreated infected SCID mice. In contrast, rare infected neurons were detected following the transfer of PKO CD8⁺ T cells, despite a similar tissue distribution to that of wt donor CD8⁺ T cells. Infected neurons are detected only in the CNS of immunodeficient mice infected with this JHMV variant, suggesting that in contrast to IFN- γ -dependent protection of neurons following alphavirus infections (6), perforin-mediated cytolysis may play a role in preventing and/or limiting JHMV infection of neurons.

JHMV infection induces MHC class I expression on oligodendroglia (26). However, the ability of PKO mice, as well as PKO/GKO recipients of PKO CD8⁺ T cells, to control virus replication in oligodendroglia suggested that an effector mechanism other than class I-dependent perforin-mediated cytolysis regulates virus infection in this cell type (5, 21). IFN- γ mRNA levels peak in the CNS coincident with virus clearance (21), but they never return to the baseline. Continuous antigen-specific T-cell activation is consistent with the retention of CD8⁺ T cells expressing an activated phenotype within the CNS following JHMV clearance (3, 19). Furthermore, during JHMV reactivation in mice deficient in humoral immunity, IFN- γ RNA remains elevated concomitant with increased virus replication (16), although ex vivo cytolytic activity remains undetectable (4, 25). An examination of JHMV pathogenesis in both GKO mice and PKO/GKO recipients of GKO CD8⁺ T cells demonstrated that IFN- γ was not only critical to survival and virus control, but that the virus replicated almost exclusively in oligodendroglia in its absence (5, 21). Although a variety of CNS-infiltrating cells can potentially secrete IFN- γ (8, 39), the effectiveness of IFN- γ -competent CD8⁺ T cells was demonstrated by virus control in oligodendroglia of PKO/GKO recipients (5). In contrast, an inability of CD8⁺ T cells to secrete IFN- γ prevents the long-term control of virus replication, similar to JHMV pathogenesis in GKO mice (21). A prominent role of IFN- γ secretion by CD8⁺ T cells was confirmed by class II induction on microglia. Unlike class I expression, class II expression on microglia is absolutely IFN- γ dependent (5, 29). The expression of class I, but not class II, molecules on microglia in untreated infected SCID mice fur-

ther suggests that infiltrating NK cells secrete insufficient IFN- γ to initiate and/or sustain class II surface expression. In contrast, the decreased expression of class I molecules on microglia in GKO CD8⁺-T-cell recipients, which harbored barely detectable NK cells by day 10 p.i. compared to untreated SCID mice, suggested that NK-cell-derived IFN- γ may help to sustain class I expression. Alternatively, virus-induced increased IFN- α/β in untreated SCID mice may enhance class I expression. The latter notion is supported by class I upregulation on microglia in infected GKO/PKO mice (5).

It has been suggested that microglia mediate CNS demyelination in the absence of infiltrating macrophages (43). The absence of demyelination in infected SCID mice and SCID recipients of GKO CD8⁺ T cells, which harbor both activated class I⁺ microglia and infiltrating class II⁺ macrophages, is inconsistent with this notion. Furthermore, the myelin loss induced by wt CD8⁺ T cells was associated with the enhanced recruitment of class II⁺ macrophages, suggesting that CNS-infiltrating macrophages contribute to JHMV-induced demyelination (5, 23, 24). However, the absence of demyelination in SCID recipients of PKO CD8⁺ T cells, despite the considerable presence of class II⁺ macrophages within the CNS, indicates that tissue damage possibly associated with cytolysis and phagocytosis is necessary, in addition to IFN- γ , to achieve an activation threshold resulting in demyelination. This is supported by the observation that uncontrolled CNS virus replication, predominantly in oligodendroglia of SCID mice, even in the presence of CD8⁺ T cells that are unable to secrete IFN- γ , is insufficient to initiate demyelination. CD4⁺ T cells may also provide an accessory component for demyelination, as indicated by demyelination in infected PKO mice and by adoptive transfer studies in JHMV-infected Rag1^{-/-} mice (5, 42).

These data demonstrate that virus-specific CD8⁺ T cells can control JHMV replication in the absence of CD4⁺ T cells. Furthermore, they provide additional evidence that perforin-mediated cytolysis and IFN- γ secretion act in concert to provide optimal control of JHMV replication in the CNS. Finally, the perforin-dependent control of virus replication in astrocytes, and potentially neurons, but IFN- γ -dependent control in oligodendroglia, the cell type which synthesizes and maintains myelin, highlights cell-type-specific susceptibilities to distinct CD8⁺-T-cell functions.

ACKNOWLEDGMENTS

This work was supported by grant NS 18146 from the National Institutes of Health. B.P. was supported by a training grant from Colciencias, Bogota, Colombia.

We thank Wen Wei and Ernesto Baron for assistance with histopathology and Maria Rameriz for breeding the mice.

REFERENCES

1. Badovinac, V. P., A. R. Tivnereim, and J. T. Harty. 2000. Regulation of antigen specific CD8⁺ T cell homeostasis by perforin and interferon- γ . *Science* **290**:1354–1358.
2. Barac-Latas, V., G. Suchanek, H. Breitschopf, A. Stuehler, H. Wege, and H. Lassmann. 1997. Patterns of oligodendrocyte pathology in coronavirus-induced subacute demyelinating encephalomyelitis in the Lewis rat. *Glia* **19**: 1–12.
3. Bergmann, C. C., J. A. Altman, D. Hinton, and S. A. Stohlman. 1999. Inverted immunodominance and impaired cytolytic function of CD8⁺ T cells during viral persistence in the central nervous system. *J. Immunol.* **163**:3379–3387.
4. Bergmann, C. C., C. Ramakrishna, M. Kornacki, and S. A. Stohlman. 2001. Impaired T cell immunity in B cell deficient mice following viral central nervous system infection. *J. Immunol.* **167**:1575–1583.
5. Bergmann, C. C., B. Parra, D. Hinton, C. Ramakrishna, M. Morrison, and S. Stohlman. 2003. Perforin mediated effector function within the CNS requires IFN- γ mediated MHC upregulation. *J. Immunol.* **170**:3204–3213.
6. Binder, G. K., and D. E. Griffin. 2001. Interferon-gamma-mediated site-specific clearance of alphavirus from CNS neurons. *Science* **293**:303–306.
7. Finke, D., U. G. Brinckmann, V. ter Meulen, and U. G. Leibert. 1995. Gamma interferon is a major mediator of antiviral defense in experimental measles virus-induced encephalitis. *J. Virol.* **69**:5469–5474.
8. Fleming, J. O., M. D. Trousdale, F. A. el-Zaatari, S. A. Stohlman, and L. P. Weiner. 1986. Pathogenicity of antigenic variants of murine coronavirus JHM selected with monoclonal antibodies. *J. Virol.* **58**:869–875.
9. Guidotti, L. G., and F. V. Chisari. 2000. Cytokine-mediated control of viral infections. *Virology* **273**:221–227.
10. Haring, J., and S. Perlman. 2001. Mouse hepatitis virus. *Curr. Opin. Microbiol.* **4**:462–466.
11. Harty, J. T., A. R. Tivnereim, and D. W. White. 2000. CD8⁺ T cell effector mechanisms in resistance to infection. *Annu. Rev. Immunol.* **18**:275–308.
12. Houtman, J. J., and J. O. Fleming. 1996. Dissociation of demyelination and viral clearance in congenitally immunodeficient mice infected with murine coronavirus JHM. *J. Neurovirol.* **2**:101–110.
13. Houtman, J. J., and J. Fleming. 1996. Pathogenesis of mouse hepatitis virus-induced demyelination. *J. Neurovirol.* **2**:361–376.
14. Kundig, T. M., H. Hengartner, and R. M. Zinkernagel. 1993. T cell-dependent IFN- γ exerts an antiviral effect in the central nervous system but not in peripheral solid organs. *J. Immunol.* **150**:2316–2321.
15. Lane, T. E., and M. J. Buchmeier. 1997. Murine coronavirus infection: a paradigm for virus-induced demyelination. *Trends Microbiol.* **5**:9–14.
16. Lin, M. T., S. A. Stohlman, and D. R. Hinton. 1997. Mouse hepatitis virus is cleared from the central nervous systems of mice lacking perforin-mediated cytolysis. *J. Virol.* **71**:383–391.
17. Lin, M. T., D. R. Hinton, N. W. Marten, C. C. Bergmann, and S. A. Stohlman. 1999. Antibody prevents virus reactivation within the central nervous system. *J. Immunol.* **162**:7358–7368.
18. Marten, N. W., S. A. Stohlman, and C. C. Bergmann. 2001. MHV infection of the CNS: mechanisms of immune-mediated control. *Viral Immunol.* **14**: 1–18.
19. Marten, N. W., S. Stohlman, and C. C. Bergmann. 2000. Role of viral persistence in retaining CD8⁺ T cells within the central nervous system. *J. Virol.* **74**:7903–7910.
20. Parra, B., D. R. Hinton, M. T. Lin, D. J. Cua, and S. A. Stohlman. 1997. Kinetics of cytokine mRNA expression in the central nervous system following lethal and nonlethal coronavirus-induced acute encephalomyelitis. *Virology* **233**:260–270.
21. Parra, B., D. R. Hinton, N. Marten, C. C. Bergmann, M. Lin, C. Yang, and S. A. Stohlman. 1999. Gamma interferon is required for viral clearance from central nervous system oligodendroglia. *J. Immunol.* **162**:1641–1647.
22. Parra, B., M. Lin, S. Stohlman, C. C. Bergmann, R. Atkinson, and D. Hinton. 2000. Contributions of Fas-Fas ligand interactions to the pathogenesis of mouse hepatitis virus in the central nervous system. *J. Virol.* **74**:2447–2450.
23. Pewe, L., and S. Perlman. 2002. Cutting edge: CD8 T cell-mediated demyelination is IFN- γ dependent in mice infected with a neurotropic coronavirus. *J. Immunol.* **168**:1547–1551.
24. Pewe, L., J. Haring, and S. Perlman. 2002. CD4 T-cell-mediated demyelination is increased in the absence of gamma interferon in mice infected with mouse hepatitis virus. *J. Virol.* **76**:7329–7333.
25. Ramakrishna, C., S. Stohlman, R. Atkinson, M. Schlomchik, and C. C. Bergmann. 2002. Mechanisms of central nervous system viral persistence: critical role of antibody and B cells. *J. Immunol.* **168**:1204–1211.
26. Redwine, J. M., M. J. Buchmeier, and C. F. Evans. 2001. In vivo expression of major histocompatibility complex molecules on oligodendrocytes and neurons during viral infection. *Am. J. Pathol.* **159**:1219–1224.
27. Ruby, J., and I. Ramshaw. 1991. The antiviral activity of immune CD8⁺ T cells is dependent on interferon- γ . *Lymphokine Cytokine Res.* **10**:353–358.
28. Russell, J. H. 1995. Activation-induced death of mature T cells in the regulation of immune responses. *Curr. Opin. Immunol.* **7**:382–388.
29. Sedgwick, J. D., and W. F. Hickey. 1997. Antigen presentation in the central nervous system, p. 364–379. *In* W. Keane and W. F. Hickey (ed.), *Immunology of the central nervous system*. Oxford University Press, Oxford, United Kingdom.
30. Shtrichman, R., and C. E. Samuel. 2001. The role of gamma interferon in antimicrobial immunity. *Curr. Opin. Microbiol.* **4**:251–259.
31. Spaner, D., K. Raju, B. Rabinovich, and R. G. Miller. 1999. A role for perforin in activation induced T cell death in vivo: increased expansion of allogeneic perforin deficient T cells in SCID mice. *J. Immunol.* **162**:1192–1199.
32. Stohlman, S., C. Bergmann, R. van der Veen, and D. R. Hinton. 1995. Mouse hepatitis virus-specific cytotoxic T lymphocytes protect from lethal infection without eliminating virus from the central nervous system. *J. Virol.* **69**:684–694.

33. **Stohlman, S. A., D. R. Hinton, D. Cua, E. Dimacali, J. Sensintaffar, F. M. Hofman, S. M. Tahara, and Q. Yao.** 1995. Tumor necrosis factor expression during mouse hepatitis virus-induced demyelinating encephalomyelitis. *J. Virol.* **69**:5898–5903.
34. **Stohlman, S. A., C. C. Bergmann, M. T. Lin, D. Cua, and D. R. Hinton.** 1998. Cytotoxic T lymphocyte effector function within the central nervous system requires CD4⁺ T cells. *J. Immunol.* **160**:2896–2904.
35. **Stohlman, S. A., and D. R. Hinton.** 2001. Viral induced demyelination. *Brain Pathol.* **11**:92–106.
36. **Sussman, M., R. Shubin, S. Kyuwa, and S. A. Stohlman.** 1989. T-cell-mediated clearance of mouse hepatitis virus strain JHM from the central nervous system. *J. Virol.* **63**:3051–3059.
37. **Tishon, A., H. Lewicki, G. Rall, M. von Herrath, and M. B. Oldstone.** 1995. An essential role for type 1 interferon-gamma in terminating persistent viral infection. *Virology* **212**:244–250.
38. **Wang, F. I., D. R. Hinton, W. Gilmore, M. D. Trousdale, and J. O. Fleming.** 1992. Sequential infection of glial cells by the murine hepatitis virus JHM strain (MHV-4) leads to a characteristic distribution of demyelination. *Lab. Invest.* **66**:744–754.
39. **Weidinger, G., G. Henning, V. ter Meulen, and S. Neiwiesk.** 2001. Inhibition of major histocompatibility class II dependent antigen presentation by neutralization of gamma interferon leads to breakdown of resistance to measles virus-induced encephalitis. *J. Virol.* **75**:3059–3065.
40. **Williamson, J. S. P., and S. A. Stohlman.** 1990. Effective clearance of mouse hepatitis virus from the central nervous system requires both CD4⁺ and CD8⁺ T cells. *J. Virol.* **64**:4589–4592.
41. **Wodarz, D., J. P. Christensen, and A. R. Thomsen.** 2000. The importance of lytic and nonlytic immune responses in viral infections. *Trends Immunol.* **23**:194–200.
42. **Wu, G. F., A. A. Dandekar, L. Pewe, and S. Perlman.** 2000. CD4 and CD8 T cells have redundant but not identical roles in virus-induced demyelination. *J. Immunol.* **165**:2278–2286.
43. **Xue, S., N. Sun, N. van Rooijen, and S. Perlman.** 1999. Depletion of blood-borne macrophages does not reduce demyelination in mice infected with a neurotropic coronavirus. *J. Virol.* **73**:6327–6334.
44. **Zhou, J., S. Stohlman, R. Atkinson, D. Hinton, and N. Marten.** 2003. Neutrophils promote mononuclear cell infiltration during viral-induced encephalitis. *J. Immunol.* **170**:3331–3336.